MODELLING OF ELECTROSTATIC TURBULENCE AT THE EDGE OF THE CASTOR TOKAMAK

K. Dyabilin[*)], R. Klíma, I. Ďuran, J. Horáček, M. Hron, P. Pavlo, J. Stöckel, F. Žáček

Institute of Plasma Physics, Association EURATOM/IPP.CR, Prague, Czech Republic
[*)]Institute of High Energy Density, Moscow, Russian Federation

Electrostatic drift wave turbulence of the CASTOR tokamak edge plasma is simulated by using the Hasegawa – Wakatani [1] equations. Sheared poloidal plasma rotation is taken into account by means of a fluid model of the plasma polarization.

Modelling is performed for the experimental conditions of the CASTOR tokamak with the aspect ratio R/a = 40 cm/8.5 cm, B_t = 1 T, I_p = 10÷15 kA. Typical central ion and electron temperatures are 50÷70 eV and 150÷200 eV, respectively, line average density 10^{19} m^{-3}. In the simulations, the region of the edge contained plasma and of the limiter shadow is considered (6 cm < r < 10 cm). The simulations yield the temporal evolution and spatial distribution of the electric potential and plasma density fluctuations. Then, the radial profiles of rms values of fluctuating quantities, their power spectra and the spatial correlation lengths are derived. Finally, the fluctuation-induced particle flux is computed. The results are compared with the experimental data obtained on the CASTOR tokamak using the 2-D matrix of Langmuir probes [2].

Theoretical Model - Basic Equations

Normalized equations for the particle density perturbation n, the potential fluctuation ϕ and vorticity w are generalized for the whole poloidal range:

$$\frac{\partial n}{\partial t}+(\nabla\phi\times\nabla n)_{\parallel} = \frac{\partial n_0}{\partial x}\frac{\partial \phi}{\partial y}-V_\theta\frac{\partial n}{\partial y}+\sigma_2 n_0\left(\frac{\phi}{T_e}-\frac{n}{n_0}\right)+D\nabla_\perp^2 n,$$

$$\frac{\partial w}{\partial t}+(\nabla\phi\times\nabla w)_{\parallel} = -G_b\left(\frac{\cos\theta}{n_0}\frac{\partial n}{\partial y}+\frac{\sin\theta}{n_0}\frac{\partial n}{\partial x}+\frac{n}{n_0}\left(\frac{1}{T}\frac{\partial T}{\partial x}\right)\sin\theta\right)+$$
$$+\sigma_1\left(\frac{\phi}{T_e}-\frac{n}{n_0}\right)-V_\theta\frac{\partial w}{\partial y}+\frac{\partial^2 V_\theta}{\partial x^2}\frac{\partial\phi}{\partial y}+\mu\nabla_\perp^2 w,$$

$$w = (\nabla\times\mathbf{v})_{\parallel}\approx\nabla_\perp^2\phi$$

where $\sigma_1=\dfrac{\omega_{ci}^2 v_{T_e}^2}{\nu_{ei}L_{\parallel}^2}\tau_0$, $\sigma_2=\dfrac{v_{T_e}^2}{\nu_{ei}L_{\parallel}^2}\tau_0$, $G_b=\dfrac{c_s^2}{x_0 R}\tau_0^2$, $T=T_e+T_i$.

According to the CASTOR geometry and typical plasma parameters, we use the following normalization

$x, y \to x/x_o$, y/x$_o$, $t\to t/\tau_o$, $\phi\to e\phi/T_o$, $T_e\to T_e/T_o$; $\tau_o = x_o^2/(T_o/eB)$, where x_o = 5 mm, T_o = 25 eV. For the magnetic field B = 1 T, the characteristic time τ_0 = 1 μs. Boundary conditions for all variables are zero for both $r = r_{min}$ and $r = r_{max.}$, and periodic in the poloidal direction. The parallel scale length $L_{\parallel}$ in the scrape-off-layer is obviously given by the circumference of the torus; in the confinement region ($r < a$), $L_{\parallel} = 2\pi Rq$ was assumed. The safety factor $q(r)$ is calculated from the ohmic current profile for Spitzer resistivity and given $T_e(r)$.

Poloidal plasma flow velocity is obtained by solving the equation for the poloidal ion force balance [3].

The system of equations is solved on a rectangular grid of 100×1256 points corresponding to the radial and poloidal directions. The grid is uniform in both directions. The radial coordinates extend from $r = 0.06$m up to $r = 0.1$m and the poloidal angle is $0 < \theta < 2\pi$.

Results

The snap-shots of the density and potential structures in the regime of saturated turbulence are shown on Fig.1. It is seen that they are of a similar character, which is obviously because of their strong coupling. Such saturated level of turbulence is observed hundreds of microseconds (for the CASTOR case) after beginning the computation. In accordance with the unfavorable curvature of the magnetic field lines, the turbulent structures appear at first in the low field side region of the torus, $-\pi/2 < \theta < \pi/2$. Then, they are redistributed poloidally, reaching a dynamic equilibrium. However, the poloidal asymmetry remains not only in the "in-out" direction, but it develops also in the "top-bottom" direction.

Local radial particle flux induced by the density and potential fluctuations can be estimated as

$$nv_r = (n_0(x) + \tilde{n}) \frac{(B \times \nabla \tilde{\phi})_r}{B^2}.$$

The simulations show that the strong outward local flux is concentrated at the low field side and tends to zero at the high field side of the torus. The flux appears to be negative (inward) at some poloidal angles, however, the poloidal average is always positive. Temporal behaviour of the poloidally averaged particle flux is shown in Fig.2a, for two different radial positions. Characteristic time of fluctuations is in the range of tens microseconds. Radial profile of the flux, averaged over time and poloidal angle is shown in Fig.2b. In the vicinity of the separatrix, the flux decreases nearly three times as compared with that in the confinement region. It should be noted that the global particle confinement time on the CASTOR tokamak is 1÷2 ms. This implies the global particle flux across the separatrix in the range of $(2\div4) \times 10^{20}$m^{-2} s^{-1}. As seen from Fig.2b, the numerical simulation yields values close to that numbers.

The spectral analysis of fluctuation data, computed at the separatrix ($r = 85$ mm), are presented in Fig. 3a. Three frequency bands, with the power spectrum density decaying as $f^{-\alpha}$ are apparent, the corresponding exponents being $\alpha \approx 0$, 0.83, or 4.2. Apart from the very low power spectra densities, the above mentioned exponents are close to the experimentally measured, cf. Fig. 3b.

Detailed pictures of the potential structures at the top of the torus obtained in the simulations are given in Fig. 4 a-d. The individual panels represent the situation in four consequent moments. It is seen that the characteristic poloidal and radial dimensions of potential structures are about (5÷10) mm. The poloidal and radial correlation lengths, derived from the spatial-temporal correlation analysis of the computed data are of the same range. This is in agreement with the pictures, obtained in experiments performed on the CASTOR tokamak using the 2-D matrix of Langmuir probes [2], see Fig. 4e. The matrix is positioned at the top of the torus and has the same poloidal dimension as the panels in Figs. (a-d).

Conclusions

Various experimentally studied regimes including externally polarized (biased) plasma have been simulated. The effect of the sheared poloidal plasma flow on the turbulent structures and on the resulting particle flux observed in experiments has been reproduced. Some interesting features of the turbulence become more visible from the animated simulation results (available at http://www.ipp.cas.cz/tokamak/turbmovie.html.)

Acknowledgement. Work partially supported by GACR grant #202/00/1216.

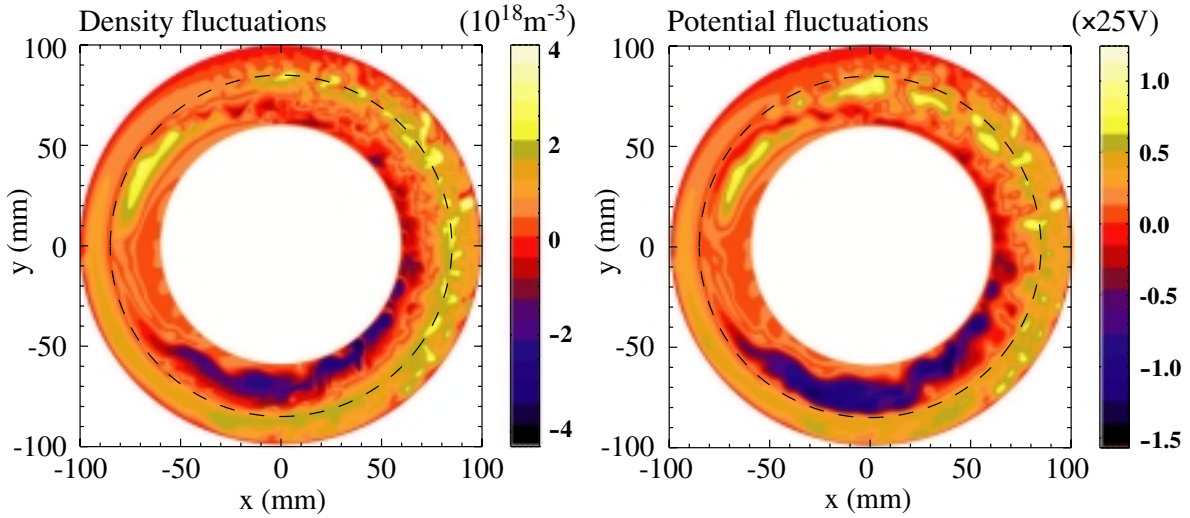

Fig. 1. *Snap-shots of turbulent structures. Left: plasma density, the scales in $10^{18}m^{-3}$. Right: plasma potential normalised to 25V.*

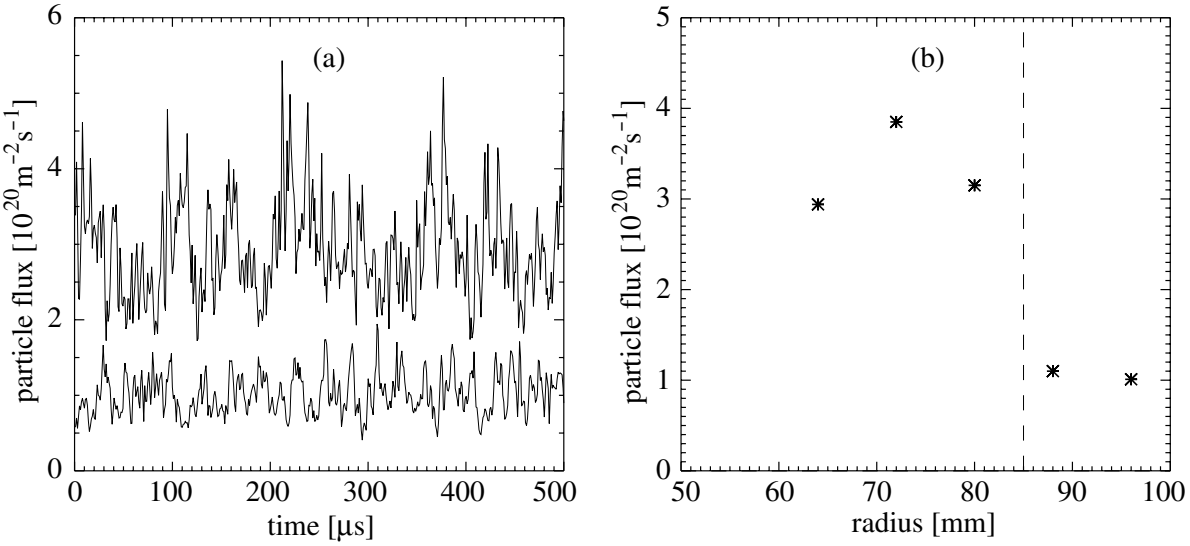

Fig. 2. *(a) Temporal evolution of the poloidally averaged particle flux. Radial positions r = 64mm (upper trace) and r = 96mm (lower trace). (b) Radial profile of the poloidally averaged particle flux.*

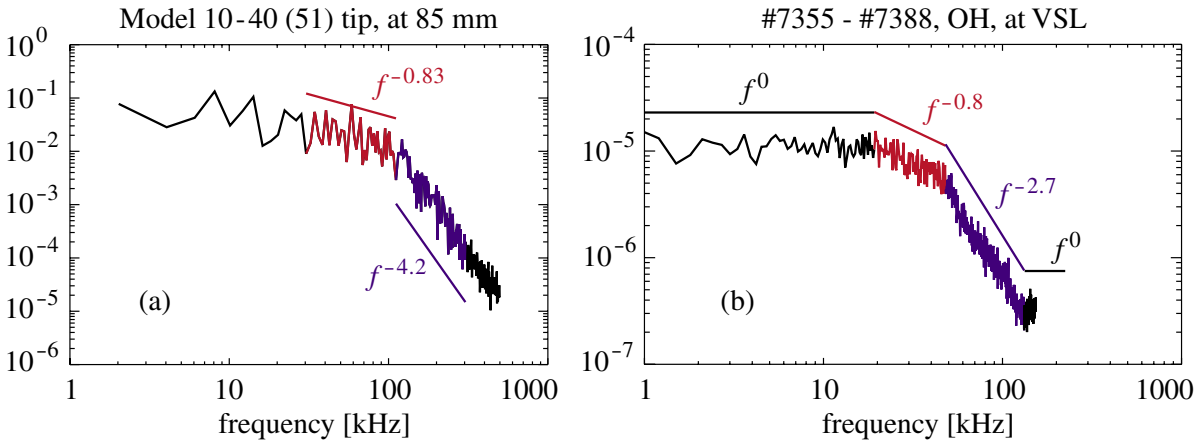

Fig. 3. *(a) Power spectra of potential fluctuations from simulation. Top of the torus, radial position r = 85 mm (separatrix). (b) Power spectrum of potential fluctuations measured at the top of the torus by a probe positioned at the separatrix (r = 85mm).*

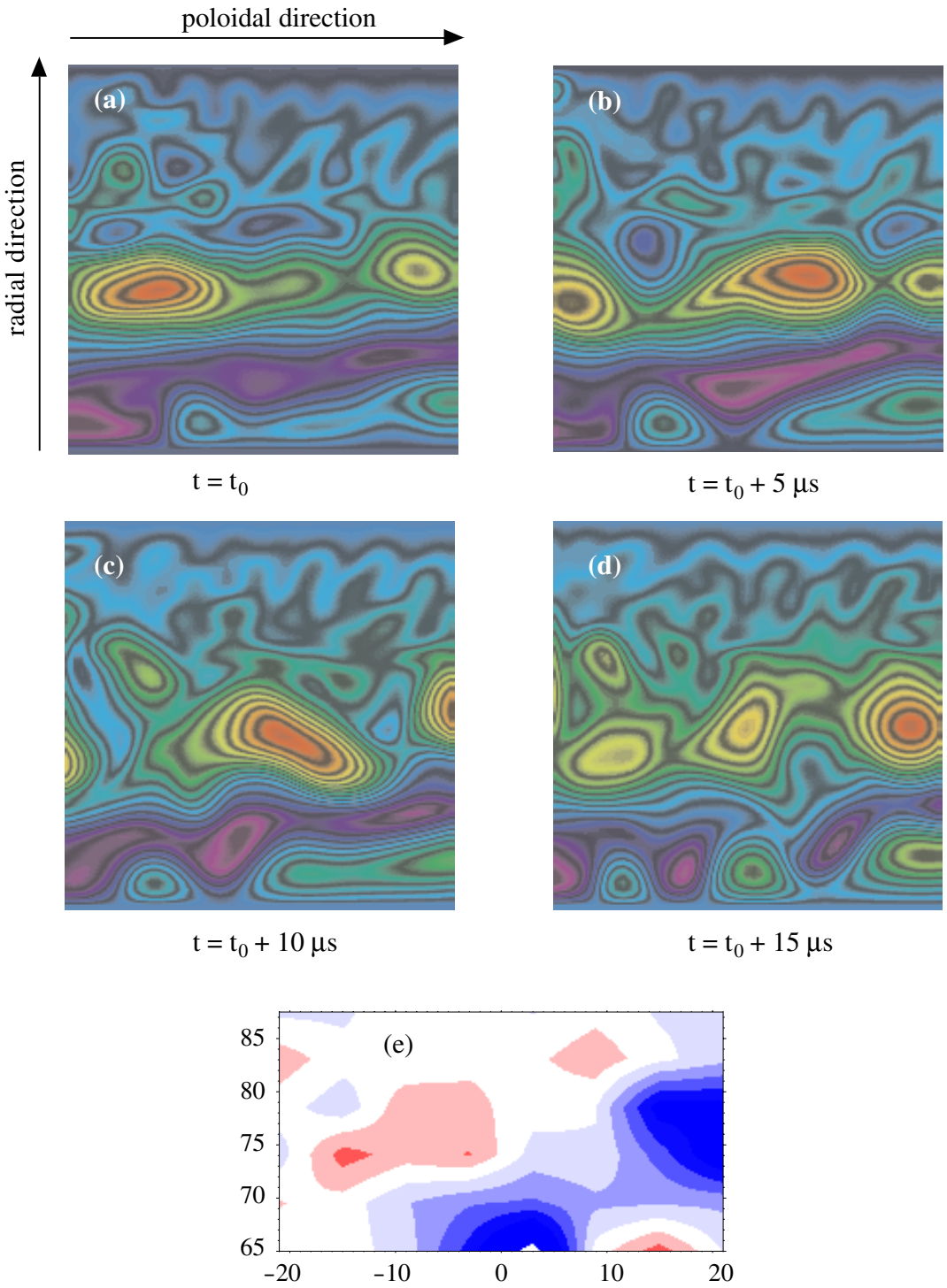

Fig. 4. *(a-d): Four snap-shots of potential structures at the top of the torus. Each panel depicts the area of 40 mm × 40 mm. (e): Potential structures measured by using 2-D matrix of Langmuir probes.*

References

[1] A. Hasegawa and M. Wakatani, Phys. Rev. Lett. **50**, 682 (1985); M. Wakatani and A. Hasegawa, Phys. Fluids **27**, 611 (1984).

[2] J. Stöckel et al., 27th EPS Conf. Contr. Fusion Plasma Phys., Budapest 2000, ECA Vol.**24B**, p. 1032.

[3] K. Dyabilin et al., Research Report IPP AS CR, Dec. 2000, IPPCZ-366.